

# Scaling Law and Aging Phenomena in the Random Energy Model

Munetaka SASAKI and Koji NEMOTO

*Division of Physics, Hokkaido University, Sapporo 060-0810*

(Received )

We study the effect of temperature shift on aging phenomena in the Random Energy Model (REM). From calculation on the correlation function and simulation on the Zero-Field-Cooled magnetization, we find that the REM satisfies a scaling relation even if temperature is shifted. Furthermore, this scaling property naturally leads to results obtained in experiment and the droplet theory.

KEYWORDS: aging, scaling, random energy model, zero-field-cooled magnetization, droplet theory

## §1. Introduction

The aging, which are dynamical behaviors largely depending on the history of system, is one of the most striking phenomena in the complex systems such as spin glasses, glasses, polymers and proteins, and has been studied vigorously from both theoretical and experimental aspects. In experiments on spin glasses, one of the most familiar methods for the study of the aging phenomena is the measurement of the Zero-Field-Cooled (ZFC) magnetization.<sup>1,2)</sup> In this measurement, the sample is quenched to a temperature  $T$  below  $T_c$  in zero field. After a waiting time  $t_w$ , a weak magnetic field is applied and the magnetization  $M(t)$  is recorded as a function of observation time  $t$ . In this experiment, the length of  $t_w$  determines the degree of equilibration and aging appears as the  $t_w$  dependence, especially, the peak of the relaxation rate  $S(t) \equiv \frac{\partial M(t)}{\partial t}$  emerges around  $t_w$  as if the system remembers how the equilibration has proceeded before the observation.

Granberg *et al.*<sup>3)</sup> modified this experiment by shifting the waiting temperature from  $T$  to  $T - \Delta T$  and observed that, although  $t_w$  was unchanged, the maximum of  $S(t)$  shifted to left with increasing  $\Delta T$  as if  $t_w$  decreased. We refer to the position of this maximum as apparent wait time  $t_w^{\text{app}}$ . This suggests that the equilibration at  $T - \Delta T$  during  $t_w$  only corresponds to the one at  $T$  during  $t_w^{\text{app}}$ . For  $\Delta T < 0$ , the position shifts to right. They also investigated the relation between  $t_w$  and  $\Delta T$  and found

$$\log(t_w^{\text{app}}/t_w) \approx -\alpha(t_w)\Delta T, \quad (1.1)$$

with the result that the coefficient  $\alpha(t_w)$  is a monotonically increasing function.

From the theoretical aspects, this phenomenon is demonstrated by the droplet theory very well,<sup>4)</sup> and is reproduced in the study of the two and three dimensional EA ising spin glass model<sup>5)</sup> and a hierarchical diffusion model.<sup>6)</sup> In this manuscript, we study this phenomenon with the Random Energy Model (REM).<sup>7,8,9)</sup> At first, we calculate a correlation function with the temperature shift and confirm that this correlation function satisfies a scaling law. Next, we carry out the simulation to observe the temperature shift ZFC magnetization. As a result, we confirm that this magnetization also satisfies the same scaling law as the correlation function, which naturally leads to the relation eq. (1.1).

The organization of this manuscript is following. In section 2, we introduce the REM. In section 3, we define the temperature shift correlation function and calculate it. In section 4, we observe the temperature shift ZFC magnetization by simulation and analyze the mechanism of this phenomenon. In section 6, we summarize this paper with some discussions.

## §2. The Random Energy Model

The REM is schematically shown in Fig. 1.<sup>7)</sup> The bottom points represent the accessible states of this system. The length of each branch represents the barrier energy  $E$ , over which the system goes from one state to another. This energy is an independent random variable distributed as

$$\rho(E)dE = \frac{dE}{T_c} \exp[-E/T_c], \quad (2.1)$$

where  $T_c$  is the transition temperature.

From the Arrhenius law, the relaxation time  $\tau(\alpha : T)$ , the average time for the system to escape from the state  $\alpha$  at  $T$ , is related to  $E(\alpha)$  as

$$\tau(\alpha : T) = \tau_0 \exp[E(\alpha)/T],$$

where  $\tau_0$  is a microscopic time scale. Hereafter  $\tau_0$  is used as the unit of time and set to 1. From eq. (2.1), the distribution of  $\tau$  can be written as

$$p_x(\tau)d\tau = \frac{x}{\tau^{x+1}}d\tau \quad (\tau \geq 1), \quad (2.2)$$

where  $x \equiv T/T_c$ . From eq. (2.2), it is easily shown that the averaged relaxation time  $\langle \tau \rangle$  is  $x/(x-1)$  for  $x > 1$  and infinite for  $x \leq 1$ . This means that the transition from the ergodic phase to the non-ergodic phase occurs at  $T_c$ .

For dynamics, we employ the following simple Markoff process. First, the system is thermally activated from  $\alpha$  in unit time with the probability

$$W(\alpha : T) = \exp[-E(\alpha)/T]. \quad (2.3)$$

Since the time evolution is Markoffian, we can easily evaluate the probability  $q(\alpha, t : T)dt$  that for the event to occur during  $t + t_0$  and  $t + t_0 + dt$  with knowing the system is in the state  $\alpha$  at  $t_0$  as

$$q(\alpha, t : T)dt = W(\alpha : T) \exp[-W(\alpha : T)t]dt. \quad (2.4)$$

We generate an event time  $t$  according to  $q(\alpha, t : T)$  to perform event-driven Monte Carlo simulation. When the magnetic field  $H$  is applied, we replace  $E(\alpha)$  in eq. (2.3) with  $E + HM_\alpha$ , where  $M_\alpha$  is the magnetization of the state  $\alpha$ . The magnetization is chosen randomly and independently from a distribution  $D(M)$  with zero mean. In this simulation, we choose the uniform distribution between  $-1$  and  $+1$  for  $D(M)$ .

After the activation, the system falls to one of all states with equal probability. In the limit  $N \rightarrow \infty$ , we can neglect the possibility that the system has stayed one state more than twice in our finite time simulation. Therefore, in this simulation, we create a new state by using the distribution functions  $\rho(E)$  and  $D(M)$  whenever activation occurs.

### §3. The Temperature Shift Correlation Function

At first, we define the correlation function mentioned in §1. This correlation function is observed in the following procedure. We consider the infinitely high temperature limit for the initial condition. In other words, the initial state is chosen randomly at  $t = 0$ . Then, the system is kept at  $T - \Delta T$  during  $t_w$  and heated (or cooled) to  $T$  after that. Here, the magnetic field  $H$  is always zero. In this procedure, we observe the correlation of magnetization between the time  $t_w$  and  $t_w + t$ , which we hereafter refer to as  $C_{\Delta T}(t, t_w)$ . It is explicitly written as

$$C_{\Delta T}(t, t_w) = \sum_{\alpha, \beta} M_\beta G_{\beta\alpha}(t) M_\alpha P_\alpha(t_w), \quad (3.1)$$

where  $P_\alpha(t_w)$  is the probability that the system is found at state  $\alpha$  at  $t_w$  and  $G_{\beta\alpha}(t)$  is the probability that the system which initially stays at  $\alpha$  reaches  $\beta$  at  $t$ . Because  $M_\alpha$  is independent random variable with zero mean, eq. (3.1) is reduced to the autocorrelation function by taking the average over the distribution of the magnetization:

$$C_{\Delta T}(t, t_w) = \overline{M^2} \sum_{\alpha} G_{\alpha\alpha}(t) P_\alpha(t_w), \quad (3.2)$$

where  $\overline{M^2}$  is the variance of the distribution  $D(M)$ . Finally, we ignore the possibility that the system is activated from  $\alpha$  between  $t_w$  and  $t + t_w$  and we still find the system at  $\alpha$  at time  $t + t_w$  in the limit  $N \rightarrow \infty$ . As the result, eq. (3.2) is further reduced to

$$C_{\Delta T}(t, t_w) = \overline{M^2} \sum_{\alpha} \exp[-W(\alpha : T)t] P_\alpha(t_w). \quad (3.3)$$

Bouchaud and Dean<sup>7)</sup> calculated the Laplace transformation of  $P_\alpha(t_w)$  and obtain the result,

$$\hat{P}_\alpha(E) = \frac{E^{x_1}}{N x_1 c(x_1)} \frac{\tau(\alpha : T - \Delta T)}{\{E\tau(\alpha : T - \Delta T) + 1\}}, \quad (3.4)$$

where  $x_1 \equiv \frac{T - \Delta T}{T_c}$  and

$$c(x) \equiv \Gamma(x)\Gamma(1 - x). \quad (3.5)$$

The inverse Laplace transformation of eq. (3.4) leads us to

$$P_\alpha(t_w) = \frac{1}{Nx_1c(x_1)\Gamma(x_1)} \int_0^{t_w} ds s^{x_1-1} \exp\left[-\frac{t_w-s}{\tau(\alpha:T-\Delta T)}\right]. \quad (3.6)$$

Now, let us rewrite  $W(\alpha:T)$  as

$$W(\alpha:T) = \tau(\alpha:T-\Delta T)^{-\gamma}, \quad (3.7)$$

where  $\gamma = \frac{T-\Delta T}{T}$ . Substituting this equation and eq. (3.6) into eq. (3.3), we obtain

$$C_{\Delta T}(t, t_w) = \frac{\overline{M^2}}{c(x_1)\Gamma(x_1)} \int_1^\infty d\tau \tau^{-x_1-1} \exp[-\tau^{-\gamma}t] \int_0^{t_w} ds s^{x_1-1} \exp\left[-\frac{t_w-s}{\tau}\right]. \quad (3.8)$$

By changing the variables as  $u \equiv t_w/\tau, v \equiv s/\tau$  and replacing the upper limit of  $u$ -integral with  $\infty$  in the assumption  $t_w \gg 1$ , we find the following scaling relation,

$$C_{\Delta T}(t, t_w) = \tilde{C}_{\Delta T}(t/t_s), \quad (3.9)$$

where

$$t_s = t_w^\gamma, \quad (3.10)$$

and

$$\tilde{C}_{\Delta T}(X) = \frac{\overline{M^2}}{c(x_1)\Gamma(x_1)} \int_0^\infty \frac{du}{u} \exp[-Xu^\gamma - u] \int_0^u \frac{dv}{v} v^{x_1} e^v. \quad (3.11)$$

We can easily check that for the case  $\Delta T = 0$ , this relation is reduced to the  $t/t_w$  scaling as shown in ref. 7.

Now, we are interested in the asymptotic behaviors of  $\tilde{C}_{\Delta T}(X)$  in the limit  $X \ll 1$  and  $X \gg 1$ . For  $X \gg 1$ , we obtain

$$\begin{aligned} \frac{C_{\Delta T}(t, t_w)}{\overline{M^2}} &= \frac{1}{\gamma c(x_1)\Gamma(x_1)} \int_0^\infty \frac{ds}{s} \exp[-s - (s/X)^{\frac{1}{\gamma}}] \int_0^{(s/X)^{\frac{1}{\gamma}}} \frac{dv}{v} v^{x_1} e^v \\ &\approx \frac{1}{x_1 \gamma c(x_1)\Gamma(x_1)} \int_0^\infty \frac{ds}{s} e^{-s} (s/X)^{x_1} \\ &= \frac{\Gamma(x_2)}{x_1 \gamma c(x_1)\Gamma(x_1)} X^{-x_2}, \end{aligned} \quad (3.12a)$$

where  $x_2 \equiv \frac{T}{T_c}$ . In the case  $X \ll 1$  and  $x_1 + \gamma > 1$ , we find

$$\begin{aligned} \frac{C_{\Delta T}(t, t_w)}{\overline{M^2}} &= 1 - \frac{1}{\gamma c(x_1)\Gamma(x_1)} \int_0^\infty \frac{ds}{s} \exp[-(s/X)^{\frac{1}{\gamma}}] \{1 - e^{-s}\} \int_0^{(s/X)^{\frac{1}{\gamma}}} \frac{dv}{v} v^{x_1} e^v \\ &\approx 1 - \frac{1}{\gamma c(x_1)\Gamma(x_1)} \int_0^\infty \frac{ds}{s} \{1 - e^{-s}\} (s/X)^{\frac{x_1-1}{\gamma}} \\ &= 1 - \frac{\Gamma(\frac{x_1+\gamma-1}{\gamma})}{(1-x_1)c(x_1)\Gamma(x_1)} X^{\frac{1-x_1}{\gamma}}. \end{aligned} \quad (3.12b)$$

For  $X \ll 1$  and  $x_1 + \gamma < 1$ ,

$$\begin{aligned}
\frac{C_{\Delta T}(t, t_w)}{M^2} &= 1 - \frac{1}{c(x_1)\Gamma(x_1)} \int_0^1 \frac{ds}{s} s^{x_1} \int_0^\infty \frac{du}{u} u^{x_1} e^{-u(1-s)} \{1 - \exp[-Xu^\gamma]\} \\
&\approx 1 - \frac{X}{c(x_1)\Gamma(x_1)} \int_0^1 \frac{ds}{s} s^{x_1} \int_0^\infty \frac{du}{u} u^{x_1+\gamma} e^{-u(1-s)} \\
&= 1 - \frac{c(x_1 + \gamma)}{c(x_1)} X.
\end{aligned} \tag{3.12c}$$

Next, we evaluate eq. (3.3) by simulation to check the validity of these results. Random average is taken over  $10^6$  samples. In this simulation, we fix  $x_1$  to 0.4 and change  $x_2$  and  $t_w$  as 0.2, 0.4, 0.6, 0.8, 1.2 and 10,  $10^2$ ,  $10^3$ ,  $10^4$ ,  $10^5$ , respectively. In Fig. 2, the scaling plot for all  $x_2$  is shown for (a)  $t/t_S \gg 1$  and (b)  $t/t_S \ll 1$ . We can see that the scaling holds very well and the exponent in eqs. (3.12a), (3.12b) and (3.12c) are rather correct, although a little deviation is observed on the coefficients for  $t/t_S \ll 1$ .

#### §4. The Result of the Temperature Shift ZFC Simulation

In this section, we show the result of simulations on the temperature shift ZFC magnetization with  $T_c = 1.0$  and  $T = 0.5$ . The number of samples for random average is  $5 \times 10^7$ . The amplitude of field is 0.1. We prepare the initial condition in the infinitely high temperature limit, the same as the temperature shift correlation function. During  $t_w$ , the temperature of the system is kept at  $T - \Delta T$ . After that, the temperature is changed to  $T$  and the field  $H$  is applied. We performed the simulations for the 36 different cases with  $t_w = 10^3, 3 \times 10^3, 10^4, 3 \times 10^4$  and  $\Delta T = 0.08, 0.06, \dots, 0, -0.02, \dots, -0.08$ .

In Fig. 3, we plot the relaxation rate  $S(t)$  for  $t_w = 3 \times 10^4$  and all  $\Delta T$ . We can see the position of the peak shifts to left with increasing  $T - \Delta T$ , although its shape becomes broader. Next, we checked whether the same scaling relation as  $C_{\Delta T}(t, t_w)$  holds or not. In Fig. 4, we plot  $S(t)$  as a function of  $t/t_S$  for all  $t_w$  and  $\Delta T$ . We can confirm the scaling law. Although the position of peak depends on  $\Delta T$  to some extent in our simulation, we consider that this dependence vanishes if we take  $\Delta T/T$  as small as that used in experiment.<sup>3)</sup> By neglecting this  $\Delta T$  dependence, we can roughly estimate the position of peak as  $t_w^{\text{app}} \approx t_S = t_w \frac{T - \Delta T}{T}$  and obtain the relation eq. (1.1) with  $\alpha(t_w) = \frac{\log(t_w)}{T}$ . This result is the same as the one from the droplet theory including the coefficient  $\alpha(t_w)$ .<sup>5)</sup>

In order to investigate how the equilibration proceeds during  $t_w$ , we examine the energy distribution  $P(E, t) (t \leq t_w)$  which is defined as the probability density that the system is found at time  $t$  in one of the states whose energy is  $E$ . In Fig. 5, we show how  $P(E, t)$  changes with time. At first sight, we can see that  $P(E, t)$  has a peak at some point  $E^*$ , which shifts to right with increasing  $t$ . The value of  $E^*$  is roughly determined how far the system can be activated during time interval  $t$ , and estimated as

$$E^* \approx T \log t. \tag{4.1}$$

For  $E \leq E^*$  the distribution is well equilibrated, so that the exponent  $\alpha_1$  is given as

$$\alpha_1 = \frac{1}{T} - \frac{1}{T_c}. \quad (4.2)$$

Note that this exponent changes its sign at  $T = T_c$ . While, the other part  $E > E^*$  is not equilibrated and the exponent  $\alpha_2$  is equal to that of  $\rho(E)$ , i.e.,

$$\alpha_2 = -\frac{1}{T_c}. \quad (4.3)$$

Equation (4.1) suggests that the speed of the peak shift varies with the temperature. In Fig. 6, we show  $P(E, t)$  for  $t = 10^4$  and all  $\Delta T$ . We can see that the position of the peak shifts to right just as Fig. 3. From these nature of  $P(E, t)$ , we understand the relation eq. (1.1) as follows: During  $t_w$  at  $T - \Delta T$ , the peak shifts to  $E^* \approx (T - \Delta T) \log(t_w)$ . We can expect that, in this experiment, the magnetization most strongly changes at the time scale in which the system can be activated to  $E^*$  at  $T$ . Therefore, we can estimate  $t_w^{\text{app}}$  from the condition

$$(T - \Delta T) \log(t_w) \approx T \log(t_w^{\text{app}}), \quad (4.4)$$

which leads to eq. (1.1) with  $\alpha(t_w) = \frac{\log(t_w)}{T}$ , as mentioned above.

## §5. Summary and Discussions

We have shown that the REM satisfies a scaling law even if the temperature is shifted and time  $t$  is scaled by  $t_S = t_w^{1 - \frac{\Delta T}{T}}$ . For the case  $\Delta T = 0$ ,  $t/t_w$ -type scaling is reported in the experiment<sup>10)</sup> and simulation on the three-dimensional  $\pm J$  Ising spin-glass model,<sup>11)</sup> although some systematic deviations from the scaling remain on the experiment. It is interesting to check whether these systems satisfy the scaling like the REM or not.

Next, we consider why the droplet theory leads to the same result as the REM. In the droplet theory, the crossover from equilibrium relaxation to non-equilibrium one occurs when the droplet created after the field application grows to the size of the droplet created before that, and we can expect that peak of  $S(t)$  emerges there. Therefore,  $t_w^{\text{app}}$  is determined by the condition

$$L(t_w, T - \Delta T) \approx L(t_w^{\text{app}}, T), \quad (5.1)$$

where  $L(t, T)$  denotes the characteristic size of the droplet after the age  $t$  at  $T$ , and is given from the condition

$$B(T, L(t, T)) = T \log(t), \quad (5.2)$$

and  $B(T, L)$  denotes the barrier energy that the system has to overcome to create the droplet of size  $L$ , and is given as  $B(T, L) = V(T)L^\psi$  explicitly. If  $T$  dependence of  $V(T)$  is weak enough, the condition eq. (5) is reduced to eq. (4.4).

Recently it was reported that  $t_w^{\text{app}}$  converges to 0 for somewhat large  $|\Delta T|$  ( $|\Delta T/T| > 0.07$  in this experiment) regardless of its sign.<sup>12)</sup> This suggests that the equilibration at  $T - \Delta T$  does affect the

one at  $T$ . In the droplet theory,<sup>13,14)</sup> it is considered that the *chaotic* change of the equilibrium spin configuration against the temperature variation causes this phenomenon. But the REM has no reason why this phenomenon is observed. Actually, this phenomenon is not observed in our simulation even in the region  $|\Delta T/T| \leq 0.16$ . But we can show that this situation is improved by treating the Multi-layer Random Energy Model (MREM), the details of which will be presented elsewhere.<sup>15)</sup>

## Acknowledgements

We would like to thank H. Yoshino for fruitful discussions and suggestions on the manuscript. The numerical calculations were performed on an Origin 2000 at Division of Physics, Graduate school of Science, Hokkaido University.

- 
- 1) P. Svedlindh, P. Granberg, P. Nordblad, L. Lundgren and H. S. Chen: Phys. Rev B **35**(1987)268.
  - 2) L. Lundgren, P. Svedlindh and O. Beckman: Phys. Rev B **26**(1982)3990.
  - 3) P. Granberg, L. Sandlund, P. Nordblad, P. Svedlindh and L. Lundgren: Phys. Rev. B **38**(1988)7097.
  - 4) D. S. Fisher and D. A. Huse: Phys. Rev. B **38**(1988)373.
  - 5) J. O. Andersson, J. Mattsson and P. Svedlindh: Phys. Rev. B **46**(1992)8297.
  - 6) C. Shulze, K. H. Hoffmann and P. Sibani: Europhys. Lett **15**(1991)361.
  - 7) J. P. Bouchaud and D. S. Dean: J. Phys. I France **5**(1995)265.
  - 8) B. Derrida: Phys. Rev. B **24**(1981)2613.
  - 9) G. J. M. Koper and H. J. Hilhorst: Europhys. Lett **3**(1987)1213.
  - 10) E. Vincent, J. Hammann, M. Ocio, J. P. Bouchaud and L. F. Cugliandolo: *Slow dynamics and aging* (Springer-Verlag, 1996) ed. M. Rubi Sitges Conference on Glassy Systems; *cond-mat/9607224*.
  - 11) Heiko Rieger: J. Phys. A **26**(1993)L615.
  - 12) P. Nordblad and P. Svendlidh: in *Spin-glasses and random fields*, edited by A. P. Young, (World Scientific, Singapore, 1997); *cond-mat/9810314*.
  - 13) A. J. Bray and M. A. Moore: Phys. Rev. Lett **58**(1987)57.
  - 14) D. S. Fisher and D. A. Huse: Phys. Rev. Lett **56**(1986)1601.
  - 15) M. Sasaki and K. Nemoto: to be submitted to J. Phys. Soc. Jpn.

## FIGURE CAPTIONS

Fig. 1 Structure of the Random Energy Model.

Fig. 2 (a)  $C_{\Delta T}(t, t_w)$  and (b)  $1 - C_{\Delta T}(t, t_w)$  is plotted as a function of  $t/t_S$  for all  $t_w$  and  $x_2$ . Each line is the asymptotic behavior estimated in eqs. (3.12a), (3.12b) and (3.12c).

Fig. 3  $S(t)$  vs.  $t$  for  $t_w = 3 \times 10^4$  and  $\Delta T = 0.08, 0.06, \dots, 0, -0.02, \dots, -0.08$  (from left to right).

Fig. 4 The scaling plot of  $S(t)$  for all  $t_w$  and  $\Delta T$ .

Fig. 5  $P(E, t)$  for  $T = 0.5$  at  $t = 10^{0.5}, 10, \dots, 10^{3.5}$  (from left to right).

Fig. 6  $P(E, t)$  for  $t = 10^4$  and  $\Delta T = 0.08, 0.06, \dots, 0, -0.02, \dots, -0.08$  (from left to right).



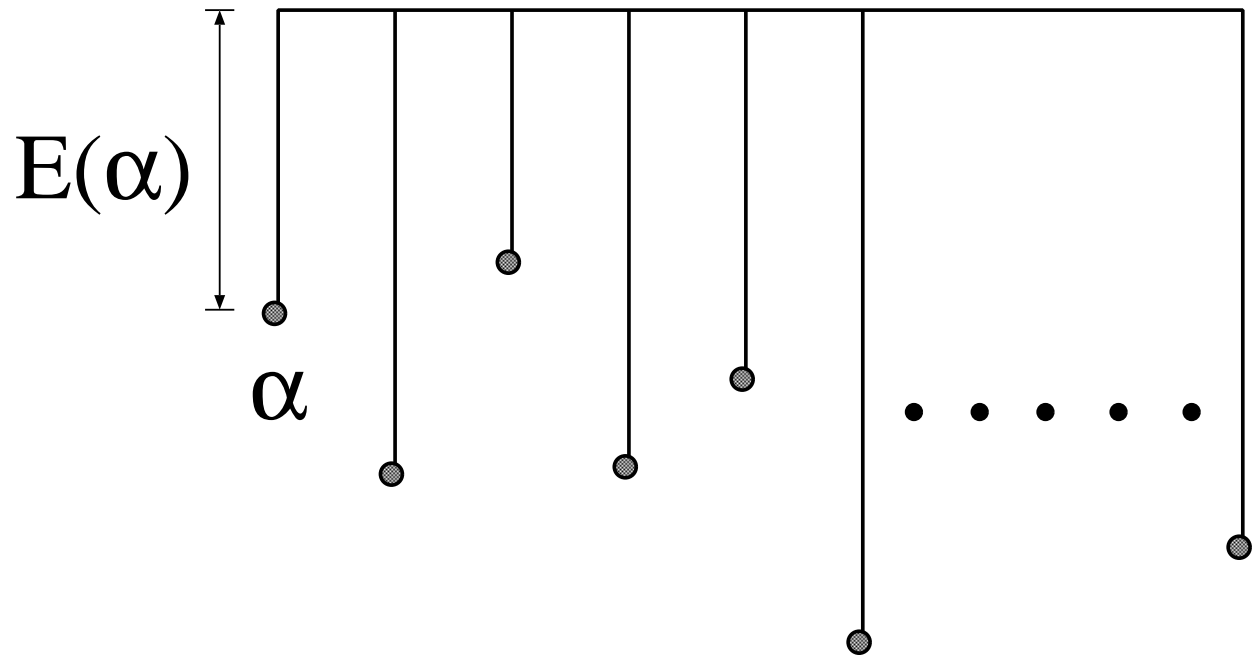


Fig. 1

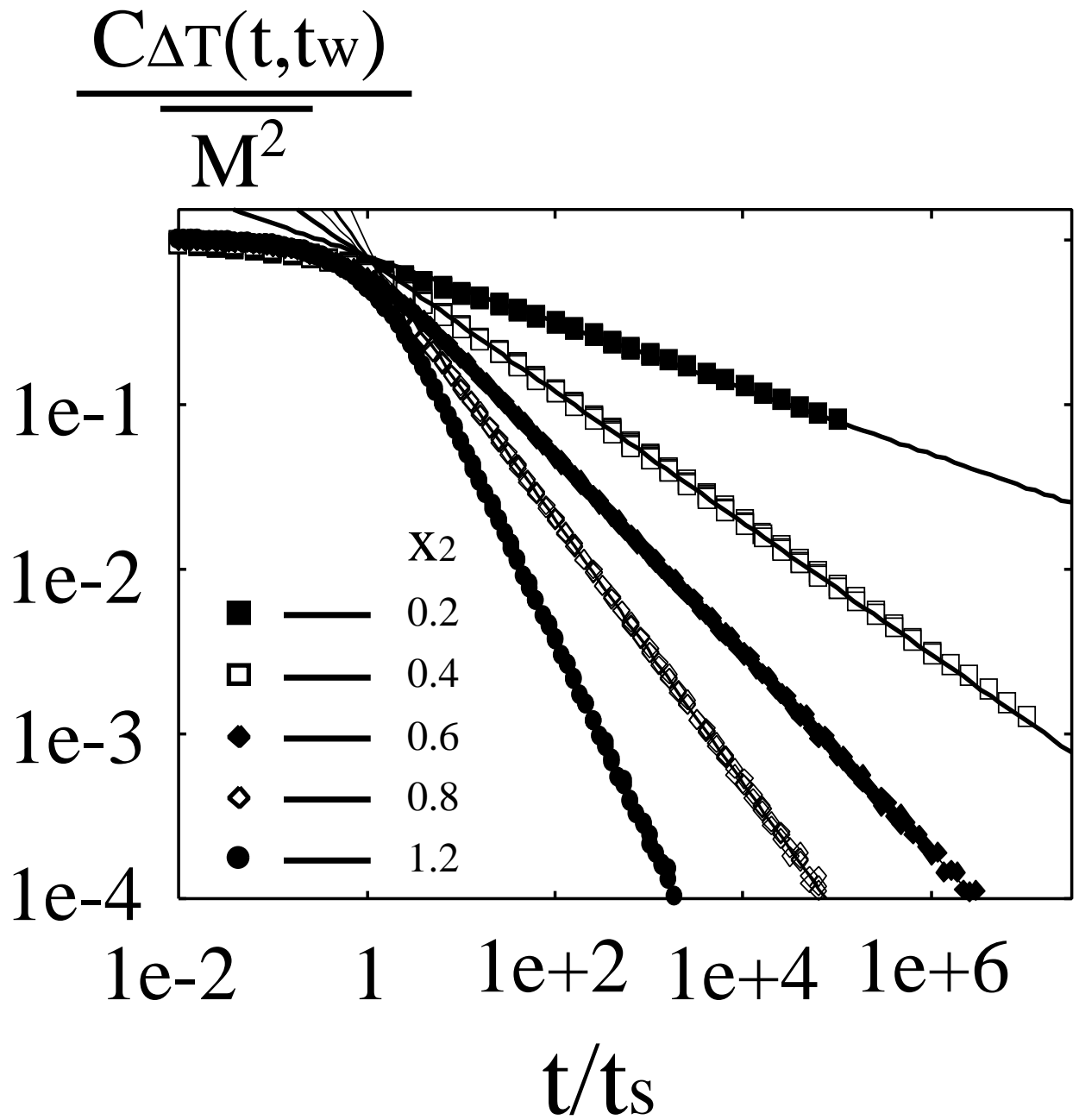


Fig. 2(a)

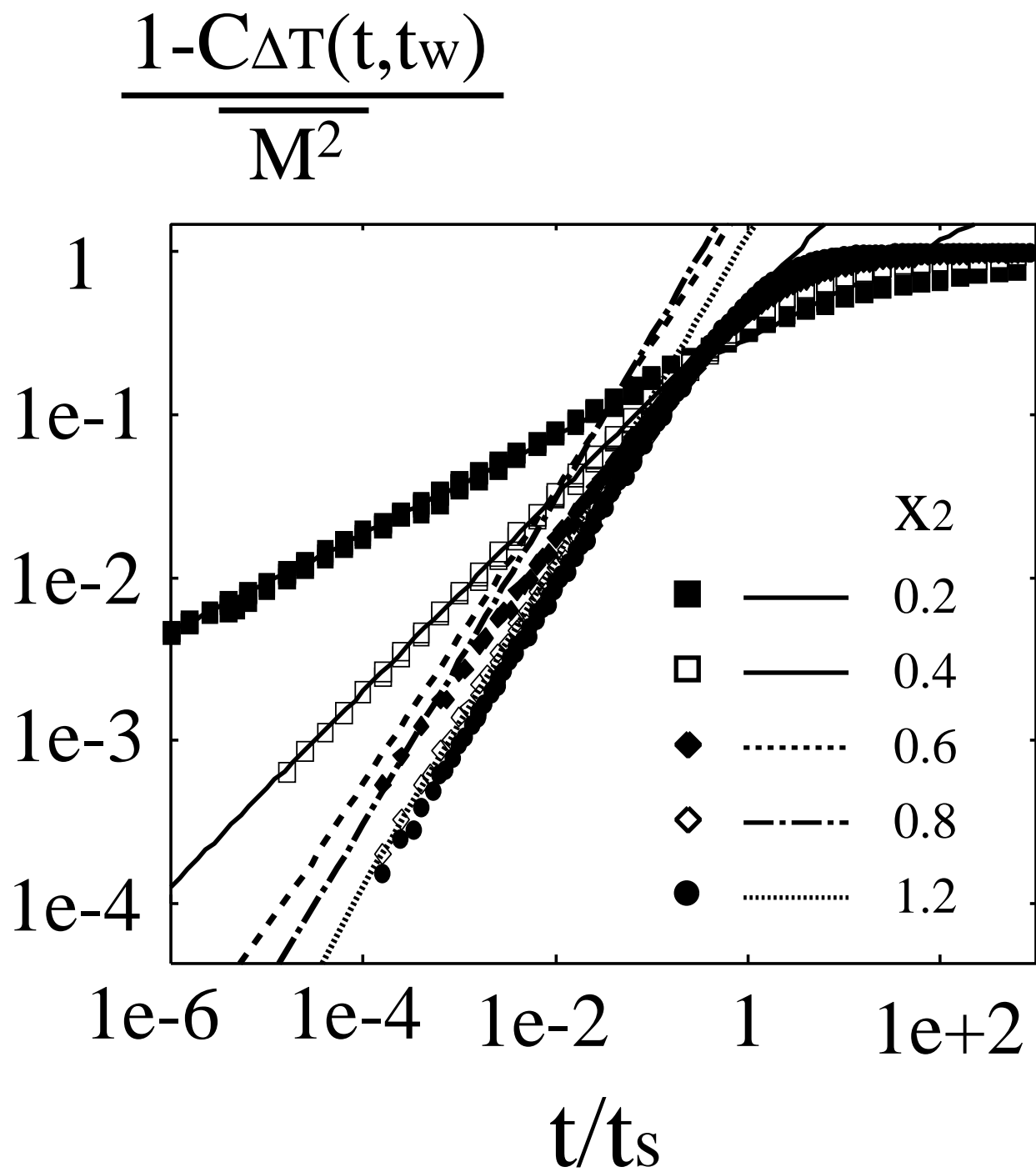


Fig. 2(b)

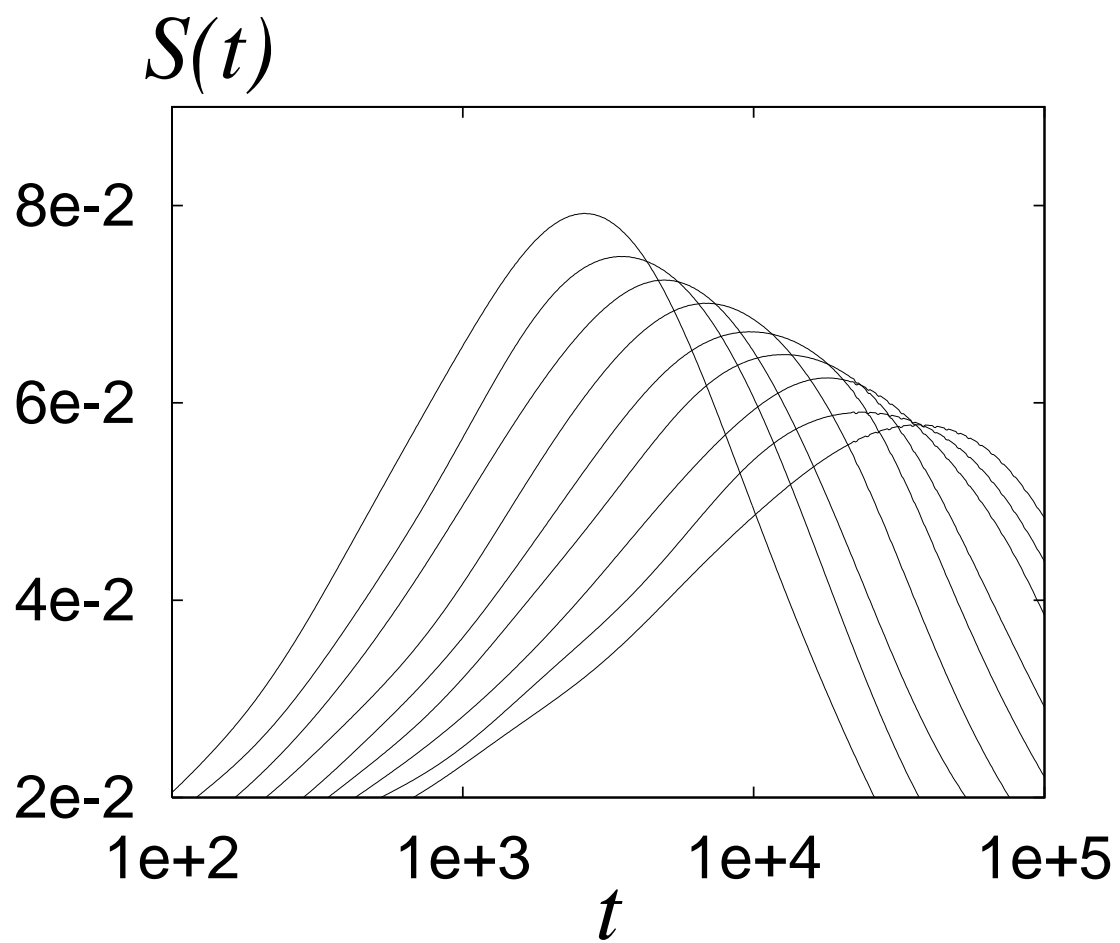


Fig. 3

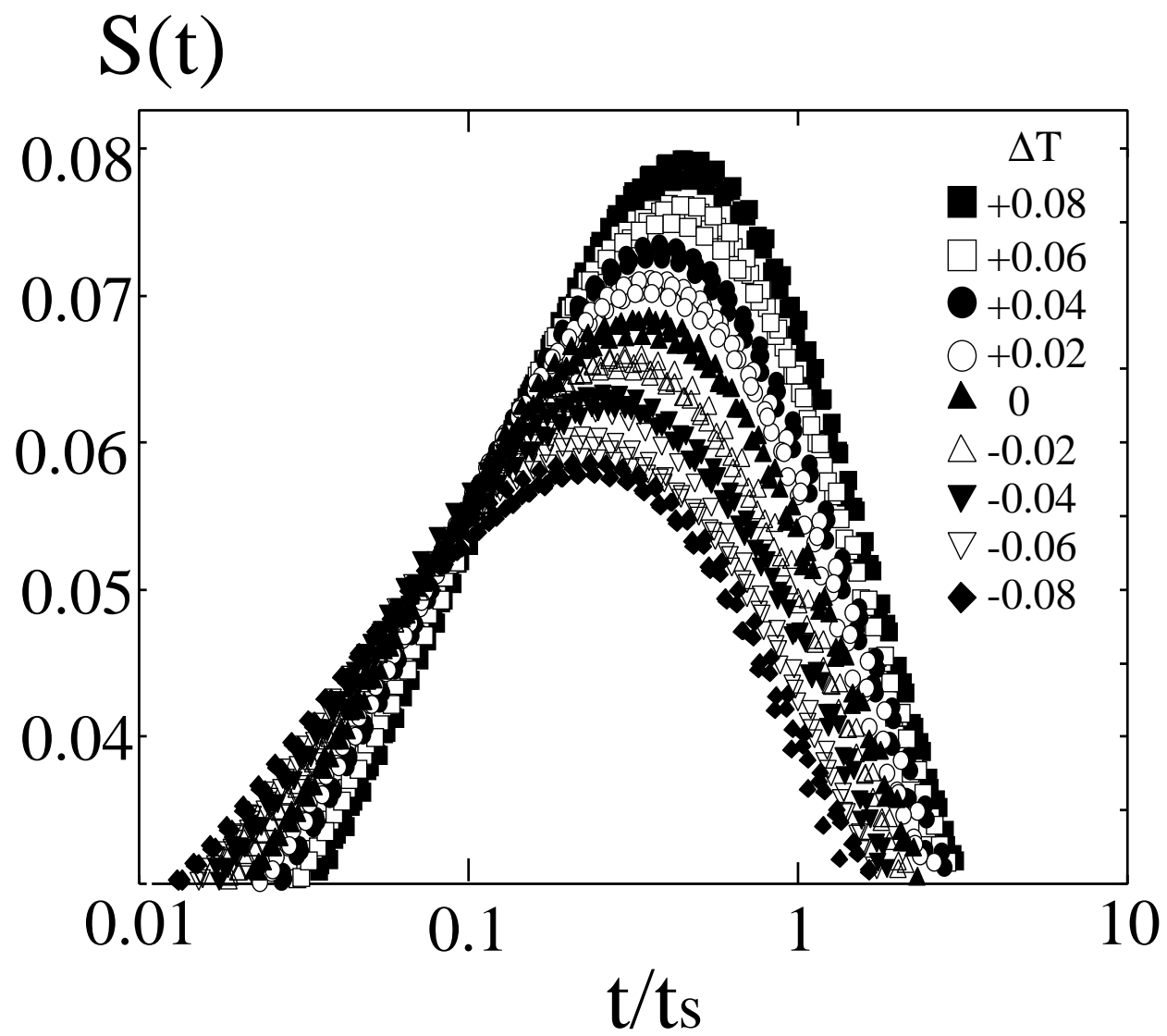


Fig. 4

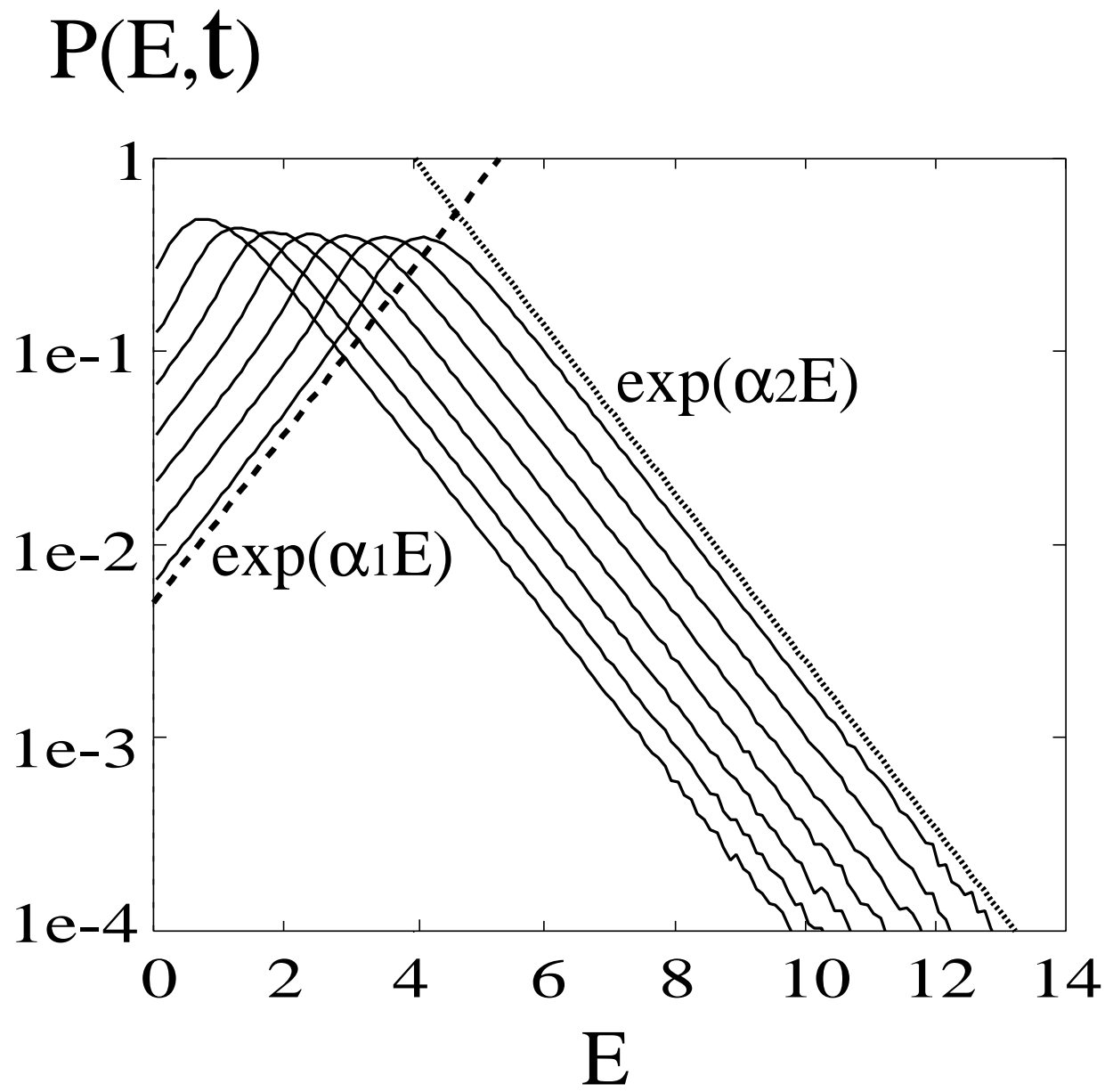


Fig. 5

$$P(E, t)$$

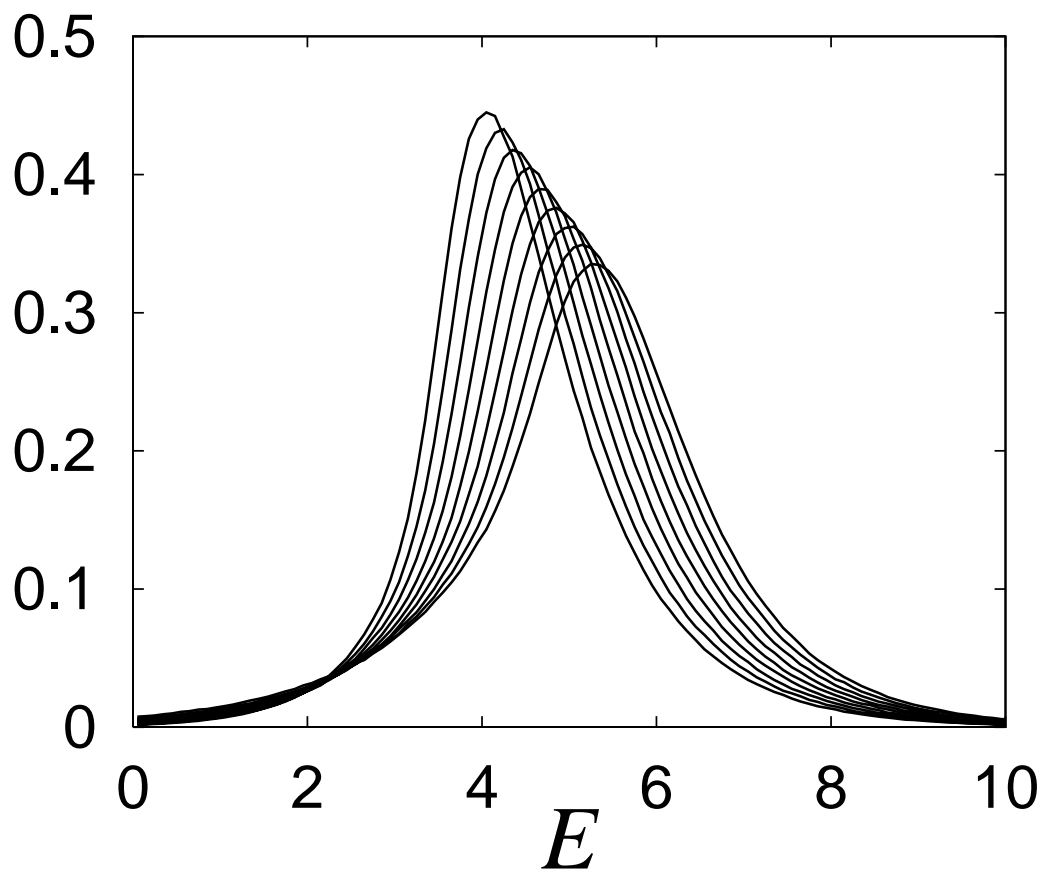


Fig. 6